

DOI 10.24425/ae.2022.140721

# An approach for electrical harmonic analysis based on interpolation DFT

LINA JIAO  , YANG DU*Shandong Polytechnic  
China**e-mail: [sdpjln@163.com](mailto:sdpjln@163.com)*

(Received: 30.08.2021, revised: 03.01.2022)

**Abstract:** The discrete Fourier transform (DFT) is the main method of electrical harmonic analysis since it's easily realized in an embedded system. But there were some difficulties in performing synchronized sampling. The spectral leakage caused by asynchronous sampling affects the accuracy of harmonics analysis. Using window functions and interpolation algorithms can improve the accuracy of harmonics analysis. An approach for electrical harmonic analysis based on the interpolation DFT was proposed. A window function reduces DFT leakage and the interpolation algorithm modifies the calculation results of frequency, amplitude and the initial phase angle. The simulation results indicate that, by using the interpolation DFT electrical harmonic analysis method based on the Hanning window or the Blackman window, the error of calculating amplitudes and frequencies is not greater than 0.5%.

**Key words:** electrical harmonic analysis, DFT, interpolation

## 1. Introduction

With the development of power electronic technology and devices, a large number of nonlinear loads are widely used in the power system. That produced many harmonic components for the power system [1–3]. A very common harmonic source is the power supply for a computer that is a switched mode power supply [4]. The access of distributed generation also produces harmonic components for the power system [5]. Harmonics worsen power quality, increase the loss of the power grid, affect weak current systems such as computer network, communication system and cable TV, and cause signal interference. The harmonic voltage will cause an unbalanced magnetic pull, and the operational stability of the PMSM will be affected to varying degrees [6]. Harmonic



© 2022. The Author(s). This is an open-access article distributed under the terms of the Creative Commons Attribution-NonCommercial-NoDerivatives License (CC BY-NC-ND 4.0, <https://creativecommons.org/licenses/by-nc-nd/4.0/>), which permits use, distribution, and reproduction in any medium, provided that the Article is properly cited, the use is non-commercial, and no modifications or adaptations are made.

distortion levels are an important index of power quality. For determining whether harmonics are present in the power system, it is necessary to study the high-precision analysis method for harmonic component parameters of the electrical system.

At present, the most direct and effective method to analyze the power system harmonic parameters is the discrete Fourier transform (DFT). Using of DFT is described in IEC 61000-4-7 [7] and IEC 61000-4-30 [8]. However, the inherent time-domain windowing and frequency-domain sampling characteristics of DFT must be selected such that the sampling frequency interval is a whole-number multiple of the frequency of the signal to be measured. If the frequency of the signal to be measured is a whole-number multiple of the sampling frequency interval, it is called synchronous sampling. If not, it is called asynchronous sampling. The asynchronous sampling is easy to cause spectrum leakage and measurement errors, especially phase errors and high-order harmonic parameter errors. There are two common methods to realize the synchronous sampling. One method is to add phase-locked synchronization technology to the acquisition system and realize synchronous sampling by hardware [9, 10]. Another method is to solve the asynchronous problem through a specific algorithm for uniformly (asynchronous) sampled data [11–14]. Suitable windows and interpolation algorithms can reduce undesirable effects due to spectral leakage caused by a sampling process that is not synchronized [15]. M. Novotny *et al.* [16] is focused on the uncertainty analysis of the RMS value and phase computed from the DFT spectrum of the noncoherently sampled signal using cosine windows.

The advantage of the former method is that the signal processing is relatively simple. However, due to the slow response speed of the phase-locked loop, it cannot track the rapid change of the signal frequency in time, so it can not realize the real synchronous sampling. The latter method has certain universality and is a common method for harmonic measurement in the power system.

The fundamental frequency (50 or 60 Hz) of the power system often fluctuates, which changes slightly with the change of loads. Even if the frequency tracking technology is adopted, it is difficult to achieve strict synchronous sampling. Aiming at this phenomenon, a DFT algorithm with spectrum-line interpolation is proposed. It is an asynchronous sampling method, which samples the signal with a fixed sampling frequency, and uses the leakage frequency generated when the window function truncates the signal to obtain the actual spectrum value of the signal. Firstly, this paper analyzes the spectrum leakage of DFT, and then, we propose an electrical harmonic analysis method based on spectrum-line interpolation DFT with the rectangular window, Hanning window and Blackman window. This method obviously reduces the impact of spectrum leakage, greatly reduces the amount of calculation, and is easy to implement in an embedded system. The simulation results show that the proposed power harmonic analysis method has high accuracy under the conditions of asynchronous sampling and non-integer period truncation.

## 2. DFT leakage

When a signal is sampled asynchronously, it is easy to cause the spectrum leakage. DFTs are constrained to operate on a finite set of  $N$  input values. Think of a continuous cosine wave with a peak amplitude of  $A$  at a frequency  $f_0$  described as:  $x(t) = A \cos(2\pi f_0 t + \varphi)$ , it is sampled at

the frequency  $f_s$  and a period of discrete-time signal is obtained as below:

$$x(n) = A \cos \left( 2\pi \left( \frac{f_0}{f_s} \right) n + \varphi \right), \quad n \in \{0, 1, \dots, N-1\}, \quad (1)$$

where:  $A$  is the peak amplitude (V) and  $A > 0$ ,  $f_0$  is the frequency of the cosine wave (Hz),  $\varphi$  is the phase angle. The DFT of the  $x(n)$  input sequence,  $X(k)$ , is as follows:

$$X(k) = \frac{A}{2} \left( e^{j\varphi} W_R \left( 2\pi \left( \frac{k}{N} - \frac{f_0}{f_s} \right) \right) + e^{-j\varphi} W_R \left( 2\pi \left( \frac{k}{N} + \frac{f_0}{f_s} \right) \right) \right), \quad (2)$$

where

$$W_R(f) = \frac{\sin(Nf/2)}{\sin(f/2)} \left( e^{-j\frac{N-1}{2}f} \right).$$

It can be seen that (2) contains positive and negative frequencies and is symmetrically distributed. For the convenience of calculation, the negative frequency part is ignored.

$$X(k) = \frac{A}{2} e^{j\varphi} W_R \left( 2\pi \left( \frac{k}{N} - \frac{f_0}{f_s} \right) \right) \quad (3)$$

and magnitudes

$$|X(k)| = \frac{A}{2} \left| W_R \left( 2\pi \left( \frac{k}{N} - \frac{f_0}{f_s} \right) \right) \right|. \quad (4)$$

It's discrete spectrum as in Fig. 1. Take  $m = \left( \frac{k}{N} - \frac{f_0}{f_s} \right)$ , and when  $m$  is a whole number, it is synchronous sampling. The spectrum is shown in Fig. 1(a). On the contrary, if  $m$  is not a whole number, i.e. asynchronous sampling, the spectrum is as shown in Fig. 1(b).

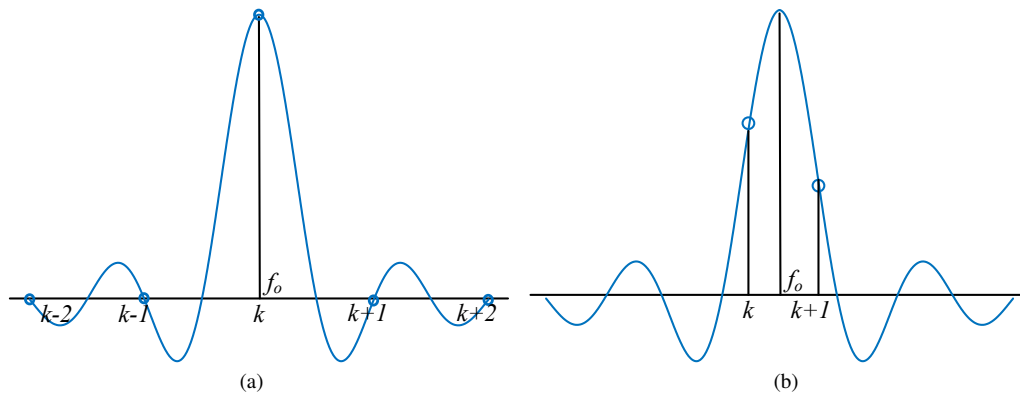


Fig. 1. Comparison of discrete spectrum: synchronous sampling (a); asynchronous sampling (b)

Spectrum leakage can be clearly seen in Fig. 1. If it is synchronous sampling, the spectrum at each discrete frequency point is consistent with the ideal spectrum of the signal, which is an ideal pulse. If it is asynchronous sampling, the spectrum at each discrete point is inconsistent with the

ideal spectrum of the signal, resulting in leakage. Therefore, the calculation results of DFT must be processed to obtain the real spectrum of the signal.

The frequency voltage or current of the power system often contains rich harmonic components, and the amplitude of harmonic components is generally a few percent or less of the fundamental component. In addition, the frequency of the power system is affected by loads, which is also a real-time variable, so it is difficult to measure synchronously. With asynchronous sampling, the spectrum leakage of fundamental components will seriously affect the calculation of harmonic components. At the same time, the harmonic components will leak to each other, resulting in the increase of harmonic analysis errors.

Although there's no way to eliminate leakage completely, we can use the method of adding windows to minimize the leakage. The window function reduces DFT leakage by minimizing the magnitude of side lobes. In fact,  $x(t) = A \cos(2\pi f_0 t + \varphi)$  is a signal of infinite length. Intercepting a section of it is equivalent to adding a rectangular window whose magnitude is 1 over the sample interval. Looking at the rectangular window's magnitude response, the main lobe width ( $-3$  dB) is  $4\pi/N$ , the maximum peak value of the side lobe is  $-13$  dB, and the asymptotic attenuation rate of the side lobe is 6 dB/octave. The amplitude of the second harmonic in the power system is generally less than 1% of the fundamental wave, that is, the amplitude attenuation of both is less than  $-40$  dB. If DFT spectrum analysis is directly used, the  $-13$  dB sidelobe will submerge the  $-40$  dB actual harmonic signal, affecting the accuracy of harmonic analysis. To reduce spectrum leakage, the window function with a small peak level of a side lobe and a large asymptotic attenuation rate of a side lobe should be selected to process the signal.

### 3. Harmonics analysis based on interpolation DFT

#### 3.1. Interpolation DFT algorithm

When using a DFT algorithm to analyze the spectrum of  $x(n)$ , it is equivalent to sampling at  $2\pi/N$  intervals in digital frequency domain. Set the digital frequency corresponding to the frequency  $f_0$  as  $(k_1 + \alpha)2\pi/N$ , where  $k_1$  is a positive integer and  $0 \leq \alpha < 1$ . That is,  $(k_1 + \alpha)2\pi f_s/N = 2\pi f_0$ . We can see that in Fig. 1(a),  $\alpha = 0$  and in Fig. 1(b),  $0 < \alpha < 1$ . Suppose that the maximum value of the discrete spectrum of the signal in Fig. 1 is at the discrete frequency points  $k_1$  and  $k_1 + 1$ , which are obtained from (4):

$$\left. \begin{aligned} |X(k)|_{k=k_1} &= \frac{A}{2} |W_R(k)|_{k=k_1} = \frac{A}{2} |W(2\pi - (\alpha)/N)| \\ |X(k)|_{k=k_1+1} &= \frac{A}{2} |W_R(k)|_{k=k_1+1} = \frac{A}{2} |W(2\pi(1 - \alpha)/N)| \end{aligned} \right\}. \quad (5)$$

Let's define

$$\beta = \frac{|X(k)|_{k=k_1+1}}{|X(k)|_{k=k_1} + |X(k)|_{k_1+1}},$$

and then

$$\beta = \frac{|X(k)|_{k=k_1+1}}{|X(k)|_{k=k_1} + |X(k)|_{k_1+1}} = \frac{|W(2\pi(1 - \alpha)/N)|}{|W(2\pi - (\alpha)/N)| + |W(2\pi(1 - \alpha)/N)|} = g(\alpha). \quad (6)$$

As a result, we can calculate  $\alpha$ .

$$\alpha = g^{-1}(\beta). \quad (7)$$

Thus, the actual frequency of the signal is estimated to be

$$f_0 = (k_1 + \alpha) \frac{f_s}{N}. \quad (8)$$

The magnitude is a correction with  $|X(k)|_{k=k_1}$ .

$$A = \frac{|X(k)|_{k=k_1}}{|W(2\pi - (\alpha)/N)|} = |X(k)|_{k=k_1} h(\alpha), \quad (9)$$

where  $\lambda$  is the correction factor of magnitude

$$\lambda = h(\alpha) = \frac{1}{|W(2\pi - (\alpha)/N)|}. \quad (10)$$

The estimation of the initial phase angle is:

$$\varphi = \text{angle}(X(k)|_{k=k_1}) - \text{angle}(W(2\pi - (\alpha)/N)). \quad (11)$$

### 3.2. Interpolation DFT without window

Directly truncating the data is equivalent to adding a rectangular window. The expression is

$$w_R(n) = 1, \quad n \in \{0, 1, \dots, N-1\}. \quad (12)$$

Further, according to the characteristics of the rectangular window, the formulas in section 3.1 are given in detail [17, 18].

$$\beta = \frac{|X(k)|_{k=k_1+1}}{|X(k)|_{k=k_1} + |X(k)|_{k=k_1+1}} = \frac{\frac{\sin(\pi(1-\alpha))}{\sin(\pi(1-\alpha)/N)}}{\frac{\sin(\pi - (\alpha))}{\sin(\pi - (\alpha)/N)} + \frac{\sin(\pi(1-\alpha))}{\sin(\pi(1-\alpha)/N)}} \approx \alpha. \quad (13)$$

So, we can get  $\alpha$

$$\alpha = g^{-1}(\beta) = \beta. \quad (14)$$

The correction factor of the magnitude  $\lambda$  is

$$\lambda = h(\alpha) = \frac{1}{|W(2\pi - (\alpha)/N)|} = \frac{2\pi\alpha}{N \sin(\pi\alpha)}. \quad (15)$$

The estimation of the initial phase angle is:

$$\varphi = \text{angle}(X(k)|_{k=k_1}) - \pi\alpha. \quad (16)$$

### 3.3. Interpolation DFT with Hanning window

To minimize the spectral leakage, we have to reduce the sidelobe magnitudes by using window functions other than the rectangular window, such as the Hanning window [17, 18]. The expression of the Hanning window function coefficient is:

$$w_{H_n}(n) = 0.5 - 0.5 \cos(2\pi n/N), \quad n \in \{0, 1, \dots, N-1\}. \quad (17)$$

The DFT of the Hanning window is as follows:

$$W_{H_n}(k) = 0.5W_R(k) + 0.25W_R(k - 2\pi/N) + 0.25W_R(k + 2\pi/N). \quad (18)$$

Assuming that our original  $N$  input signal samples  $x(n)$  as (1) is multiplied by the corresponding window  $w(n)$  coefficients before the DFT is performed. The DFT of the windowed  $x(n)$  input sequence is  $X_{H_n}(k)$ . The peak magnitude of the frequency  $X_{H_n}(k_1)$  and  $X_{H_n}(k_1 + 1)$  are:

$$|X_{H_n}(k)|_{k=k_1} \approx \frac{A}{4} \left| \frac{\sin(\pi\alpha)}{\frac{\alpha(1-\alpha)(1+\alpha)\pi}{N}} \right|, \quad (19)$$

$$|X_{H_n}(k)|_{k=k_1+1} \approx \frac{A}{4} \left| \frac{\sin(\pi\alpha)}{\frac{\alpha(1-\alpha)(2-\alpha)\pi}{N}} \right|.$$

So,

$$\beta = \frac{|X_{H_n}(k)|_{k=k_1+1}}{|X_{H_n}(k)|_{k=k_1} + |X_{H_n}(k)|_{k=k_1+1}} = \frac{(1+\alpha)}{3} \quad \text{and} \quad \alpha = -1 + 3\beta. \quad (20)$$

Similarly, it can be deduced that the amplitude  $A$  is:

$$\lambda = h(a) = \frac{4\pi\alpha(1-\alpha^2)}{N \sin(\pi\alpha)}. \quad (21)$$

The estimation of the initial phase angle is the same as the rectangle window in (15).

### 3.4. Interpolation DFT with Blackman window

Along with the Hanning window and the Hamming window, the Blackman window provides further DFT spectral leakage reduction when performing frequency-domain windowing. The Blackman window function is defined as

$$w_{B_m}(n) = 0.42 - 0.5 \cos(2\pi n/N) + 0.08 \cos(4\pi n/N), \quad n \in \{0, 1, \dots, N-1\}. \quad (22)$$

The DFT of the Blackman window:

$$W_{B_m}(k) = 0.42W_R(k) - 0.25W_R(k - 2\pi/N) - 0.25W_R(k + 2\pi/N) + 0.04W_R(k - 4\pi/N) + 0.04W_R(k + 4\pi/N). \quad (23)$$

Similarly to sections 3.1 and 3.2, the calculation expressions of  $\alpha = g^{-1}(\beta)$  can be derived. However, this process is more complex, which can be solved by polynomial approximation. First, take a group of values and substitute them into (6) to obtain a group of  $\beta$  values. Then  $\alpha = g^{-1}(\beta)$  can be obtained by using the MATLAB polynomial fitting function  $polyfit(\beta)$  coefficient. For the Blackman window, the correction factors are as follows:

$$\alpha = 2.543007\beta^5 - 6.357519\beta^4 + 7.578482\beta^3 - 5.010204\beta^2 + 5.631278\beta - 1.692522. \quad (24)$$

The amplitude calculation also needs correction. From (14), we can get an expression for  $\lambda$ . But, the expression is complex. Similarly, we can use  $\lambda = polyfit(\alpha)$  to simulate the relationship between  $\lambda$  and  $\alpha$ .

$$\begin{aligned} \lambda = & 0.428528\alpha^6 - 567764\alpha^5 + 1.139802\alpha^4 - 186457\alpha^3 \\ & + 2.426640\alpha^2 - 002771\alpha + 4.7619555. \end{aligned} \quad (25)$$

The estimation of the initial phase angle is the same as the rectangle window in (16).

#### 4. Simulation experiment verification

The 11th harmonic signal model used in the simulation is

$$x(n) = \sum_{i=1}^{11} \sqrt{2}A_i \cos\left(2\pi i \frac{f_0}{f_s} n + \varphi_i\right), \quad n \in \{0, 1, \dots, N-1\}. \quad (26)$$

where: the fundamental frequency  $f_0$  is 49.80 Hz, the sampling frequency  $f_s$  is 10 000 Hz, the total number of sampling points  $N$  is 2048,  $\sqrt{2}A_i$  is the amplitude of the fundamental wave and each harmonic,  $\varphi_i$  is the initial phase angle of the fundamental wave and each harmonic. The values of  $A_i$  and  $\varphi_i$  are shown in Table 1.

Table 1. Components of the simulated harmonic signal

Harmonics	H1	H2	H3	H4	H5	H6	H7	H8	H9	H10	H11
$f_i$ (Hz)	49.80	99.60	149.40	199.20	249.00	298.80	348.60	398.40	448.20	498.00	547.80
$A_i$ (V)	220	1.2	6.1	0.8	3.4	0.6	2.1	0.4	1.5	0.3	0.6
$\varphi_i$ (°)	10	50	30	40	50	60	70	80	90	80	60

The flow of the simulation program is presented in Fig. 2. The input signal  $x(n)$  is processed with the rectangular window, the Hamming window and the Blackman window respectively, and the discrete spectrum is obtained by DFT operation. According to the spectral line interpolation correction formula of different windows, the frequency  $f_1$ , amplitude  $A_1$  and phase angle  $\phi_1$  are calculated separately. And the frequency  $f_i$ , amplitude  $A_i$  and initial phase angle  $\phi_i$  of each harmonic are also calculated. The error percentage of the measured values of the fundamental wave and each harmonic relative to the true value is given in the Table 2. It can be seen from Table 2

that after adding the Hanning window, the calculation results are greatly improved compared with the rectangular window. After the Blackman window processing, the calculation results are ideal, except for the parameter calculation error of the second harmonic. In order to further reduce the error, it is necessary to find a better window function. However, adding a window function also increases the computational complexity. It is necessary to select the appropriate window function according to the calculation requirements and performance.

Table 2. Comparisons of relative errors in calculating (%)

Order	Without window			Hanning window			Blackman window		
	Frequency	Amplitude	Phase	Frequency	Amplitude	Phase	Frequency	Amplitude	Phase
H1	-9.1E-02	4.3E-01	4.0E+00	-7.2E-06	3.6E-05	1.3E-02	-1.1E-06	3.7E-04	5.2E-03
H2	3.1E+00	2.9E+02	1.3E+02	-6.5E-02	3.8E-01	2.9E-01	-3.3E-02	1.3E-01	6.8E-01
H3	1.4E+00	-3.3E+00	-7.9E+01	-6.7E-04	-3.8E-04	-9.6E-02	-3.5E-04	7.1E-05	-2.3E-02
H4	5.2E+00	2.0E+02	3.3E+02	-2.8E-03	-7.9E-03	-2.8E-01	-1.3E-03	-3.3E-03	-6.8E-02
H5	3.2E-01	1.2E+01	3.6E+01	5.6E-04	1.4E-02	-1.3E-01	3.1E-04	5.3E-03	-6.6E-02
H6	-2.6E-01	1.9E+02	1.6E+02	7.4E-04	2.7E-03	-2.2E-01	3.1E-04	1.8E-03	-9.2E-02
H7	-3.4E-01	1.5E+01	8.6E+01	-9.2E-05	2.1E-03	4.3E-04	-5.0E-05	5.2E-04	2.5E-03
H8	-3.2E+00	1.9E+02	-3.1E+02	-1.1E-03	1.9E-02	2.1E-02	-5.6E-04	7.1E-03	3.1E-02
H9	-6.9E-01	-8.7E+00	8.6E+01	-1.4E-05	5.6E-04	-1.2E-02	-3.2E-06	-2.8E-05	-4.9E-03
H10	-2.9E+00	1.5E+02	-3.1E+02	-2.1E-03	-8.9E-02	3.9E-01	-1.0E-03	-3.6E-02	2.0E-01
H11	2.5E+00	2.5E+01	-3.8E+02	-7.1E-05	2.2E-03	2.8E-02	-3.9E-05	1.3E-03	1.5E-02

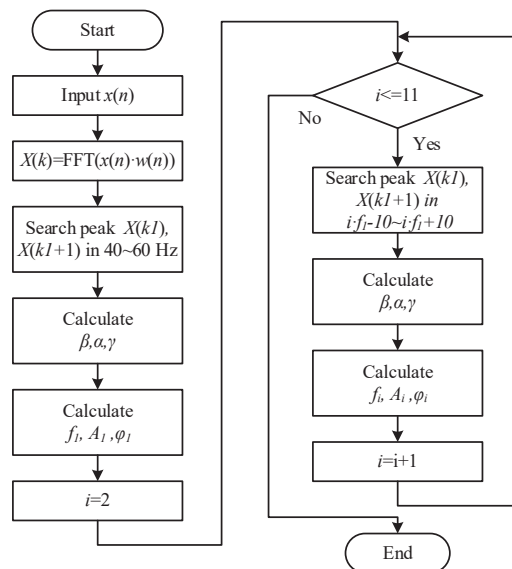


Fig. 2. Program flow diagram for simulation experiment

From the data in Table 2, we can see that for the data processed with Hanning window and Blackman window functions, the relative error of harmonic parameters is significantly smaller than that without window functions. In particular, the calculation error of frequency and amplitude is reduced to about 0.001 times. The characteristic of adding the Blackman window function is obviously better than that of adding the Hanning window function.

## 5. Conclusions

It is difficult to realize synchronous sampling because the frequency of the power system changes frequently. Asynchronous sampling DFT is usually used in power system harmonic analysis. Due to spectrum leakage, the calculation error is large. In order to avoid the error of harmonics analysis, the window function interpolation DFT algorithm is used, and the practical interpolation correction formula is obtained by using the fitting function. The simulation results show that the interpolation DFT power harmonic analysis method based on the Hanning window and the Blackman window proposed in this paper has higher calculation accuracy, less calculation and high practical value.

## References

- [1] Schlabbach J., Blume D., Stephanblome T., *Voltage quality in electrical power systems*, The Institution of Engineering and Technology (2001).
- [2] Yudaev I.V., Rud E.V., Yundin M.A., Ponomarenko T.Z., Isupova A.M., *Analysis of the harmonic composition of current in the zero-working wire at the input of the load node with the prevailing non-linear power consumers*, Archives of Electrical Engineering, vol. 70, no. 2, pp. 463–473 (2021), DOI: [10.24425/aee.2021.136996](https://doi.org/10.24425/aee.2021.136996).
- [3] Szulborski M., Kolimas L., Lapczynski S., Szczesniak P., *Single phase UPS systems loaded with nonlinear circuits: Analysis of topology in the context of electric power quality*, Archives of Electrical Engineering, vol. 68, no. 4, pp. 787–802 (2019), DOI: [10.24425/aee.2019.130683](https://doi.org/10.24425/aee.2019.130683).
- [4] Short T., *Electric Power Distribution Handbook*, Second Edition, CRC Press (2014).
- [5] Abbas A.S., El-Sehiemy R.A., Abou El-Ela A., Ali E.S., Mahmoud K., Lehtonen M., Darwish M.M.F., *Optimal harmonic mitigation in distribution systems with inverter based distributed generation*, Applied Sciences (Switzerland), vol. 11, no. 2, 774, pp. 1–16 (2021), DOI: [10.3390/app11020774](https://doi.org/10.3390/app11020774).
- [6] Geng S., Zhang Y., Qiu H., Yang C., Yi R., *Influence of harmonic voltage coupling on torque ripple of permanent magnet synchronous motor*, Archives of Electrical Engineering, vol. 68, no. 2, pp. 399–410 (2019), DOI: [10.24425/aee.2019.128276](https://doi.org/10.24425/aee.2019.128276).
- [7] IEC 61000-4-30, *Testing and measurement techniques-Power quality measurement methods*.
- [8] IEC, IEC 61000-4-7, *Testing and measurement techniques-General guide on harmonics and inter-harmonics measurements and instrumentation, for power supply systems and equipment connected thereto*.
- [9] Rodriguez P., Luna A., Candela I. et al., *Multiresonant frequency-locked loop for grid synchronization of power converters under distorted grid conditions*, IEEE Transactions on Industrial Electronics, vol. 58, no. 1, pp. 127–138 (2011), DOI: [10.1109/TIE.2010.2042420](https://doi.org/10.1109/TIE.2010.2042420).
- [10] Guo L., Wang D., Diao L., Jiang Y., Feng H., *A modified design of phase-locked loop for unbalanced and distorted grid voltage conditions*, Transactions of China Electrotechnical Society, vol. 33, no. 6, pp. 1390–1399 (2018), DOI: [10.19595/j.cnki.1000-6753.tces.170291](https://doi.org/10.19595/j.cnki.1000-6753.tces.170291).

- [11] Zhang Fusheng, Geng Zhengxing, Yuan Wei, *The algorithm of interpolating windowed FFT for harmonic analysis of electric power system*, IEEE Trans on Power Delivery, vol. 16, no. 2, pp. 160–164 (2001), DOI: [10.1109/61.915476](https://doi.org/10.1109/61.915476).
- [12] Pang Hao, Li Dongxia, Zu Yunxiao *et al.*, *An improved algorithm for harmonic analysis of power system using FFT Technique*, Proceedings of the CSEE, vol. 23, no. 6, pp. 50–54 (2003).
- [13] Xu Y., Liu Y., Li Z., Li Z., *An accurate approach for harmonic detection based on 6-term cosine window and quadruple-spectrum-line interpolation FFT*, Power System Protection and Control, vol. 44, no. 22, pp. 56–63 (2016), DOI: [10.7667/PSPC151933](https://doi.org/10.7667/PSPC151933).
- [14] Zhang C., Wang W., Qiu Y., *Detection Method of Subsynchronous Harmonic in Regions with Large Scale Wind Power Paralleled in Grid*, High Voltage Engineering, DOI: [10.13336/j.1003-6520.hve.20181207008](https://doi.org/10.13336/j.1003-6520.hve.20181207008).
- [15] Andria G., Savino M., Trotta A., *Windows and interpolation algorithms to improve electrical measurement accuracy*, IEEE Transactions on Instrumentation and Measurement, vol. 38, no. 8, pp. 856–863 (1989).
- [16] Novotny M., Slepíčka D., Sedláček M., *Uncertainty analysis of the RMS value and phase in the frequency domain by noncoherent sampling*, IEEE Transactions on Instrumentation and Measurement, vol. 56, no. 3, pp. 983–989 (2007), DOI: [10.1109/TIM.2007.894189](https://doi.org/10.1109/TIM.2007.894189).
- [17] Schoukens J., Pintelon R., Van Hamme H., *The interpolated fast Fourier transform: A comparative study*, IEEE Transactions on Instrumentation and Measurement, vol. 41, no. 2, pp. 226–232 (1992), DOI: [10.1109/19.137352](https://doi.org/10.1109/19.137352).
- [18] Agrež D., *Weighted Multi-Point Interpolated DFT to Improve Amplitude Estimation of Multi-Frequency Signal*, IEEE Transactions on Instrumentation and Measurement, vol. 51, pp. 287–292 (2002), DOI: [10.1109/19.997826](https://doi.org/10.1109/19.997826).